MOLECULAR AND CELLULAR BIOLOGY, Apr. 2010, p. 1689–1702 Vol. 30, No. 7
0270-7306/10/$12.00 doi:10.1128/MCB.01105-09

Characterization of PXK as a Protein Involved in Epidermal Growth Factor Receptor Trafficking▽

Hiroshi Takeuchi,[1] Takako Takeuchi,[1] Jing Gao,[1] Lewis C. Cantley,[2]* and Masato Hirata[1]*

Laboratory of Cellular and Molecular Biochemistry, Faculty of Dental Science, and Station for Collaborative Research, Kyushu University, Fukuoka 812-8582, Japan,[1] and Department of Systems Biology, Harvard Medical School, and Division of Signal Transduction, Department of Medicine, Beth Israel Deaconess Medical Center, Boston, Massachusetts 02115[2]

Received 18 August 2009/Returned for modification 14 September 2009/Accepted 11 January 2010

The phox homology (PX) domain is a phosphoinositide-binding module that typically binds phosphatidylinositol 3-phosphate. Out of 47 mammalian proteins containing PX domains, more than 30 are denoted sorting nexins and several of these have been implicated in internalization of cell surface proteins to the endosome, where phosphatidylinositol-3-phosphate is concentrated. Here we investigated a multimodular protein termed PXK, composed of a PX domain, a protein kinase-like domain, and a WASP homology 2 domain. We show that the PX domain of PXK localizes this protein to the endosomal membrane via binding to phosphatidylinositol 3-phosphate. PXK expression in COS7 cells accelerated the ligand-induced internalization and degradation of epidermal growth factor receptors by a mechanism requiring phosphatidylinositol 3-phosphate binding but not involving the WASP homology 2 domain. Conversely, depletion of PXK using RNA interference decreased the rate of epidermal growth factor receptor internalization and degradation. Ubiquitination of epidermal growth factor receptor by the ligand stimulation was enhanced in PXK-expressing cells. These results indicate that PXK plays a critical role in epidermal growth factor receptor trafficking through modulating ligand-induced ubiquitination of the receptor.

Both constitutive endocytosis and activated endocytosis are highly regulated events by which cells take up nutrients and internalize receptors for recycling or degradation (47). Endocytosed molecules are delivered to early endosomes, where the components are sorted to the cell surface for recycling back to the plasma membrane, or to late endosomes to be degraded in lysosomes (17). The molecular mechanisms regulating these events are not fully understood.

One of the major protein families involved in the trafficking of membrane compartments is sorting nexins (SNXs), which are characterized by the presence of phox homology (PX) domains (8, 65). The PX domain is a protein module which consists of approximately 130 amino acids with three β-strands followed by three α-helices forming a helical subdomain, and the general function of this module is to interact with the head groups of inositol phospholipids through which parental proteins are targeted to specific cellular compartments. Most of the SNXs examined to date specifically recognize phosphatidylinositol 3-phosphate [PtdIns(3)P], which is found predominately in early endosomes (11). The founding member of the SNX family, SNX1, was initially identified as an interaction partner of epidermal growth factor receptor (EGFR), and the expression of SNX1 enhanced lysosomal degradation of EGFR (38); therefore, SNXs are most likely to be involved in the trafficking of many different families of receptors which are recycled to the cell surface or sent to the lysosome for degradation (19). On the other hand, PX domain-containing proteins have also been reported to bind to phosphoinositides other than PtdIns(3)P and to have functions independent of receptor trafficking (54). For example, phospholipase D is a PX domain-containing protein that hydrolyzes phosphatidylcholine to produce a second-messenger molecule, phosphatidic acid. Interestingly, phospholipase D has been recently shown to accelerate EGFR endocytosis by activating dynamin GTPase through its PX domain but independently of lipase activity (39). Cytokine-independent survival kinase (CISK) is a PX domain-containing protein kinase that has also been shown to regulate sorting of a chemokine receptor CXCR4 through AIP4, the CXCR4 ubiquitin ligase (60). RGS-PX1, a GTPase-activating protein for Gαs of heterotrimeric GTP-binding proteins, and KIF16B, a PX domain-containing kinesin superfamily member, have been shown to regulate EGFR trafficking (27, 72) and are now grouped into the SNX family as SNX13 and SNX26, respectively.

Another feature of the PX domain is a well-conserved polyproline sequence (PXXP) in the variable loop between α1 and α2 helices, which led to the original identification of the PX domain as a SH3 domain-binding partner (53). The physiological importance of both intermolecular and intramolecular interactions mediated by polyproline sequences has been shown in various molecules, including phospholipase D2 (33) and $p47^{phox}$ (1). In mammals, there are currently 47 proteins harboring PX domains, and 30 proteins are termed SNXs (59). The functions of these proteins have just begun to be revealed.

Actin cytoskeletal dynamics have been implicated not only in

* Corresponding author. Mailing address for Lewis C. Cantley: Division of Signal Transduction, Beth Israel Deaconess Medical Center, 77 Avenue Louis Pasteur, 10th Floor, Boston, MA 02115. Phone: (617) 667-0947. Fax: (617) 667-0957. E-mail: lewis_cantley@hms.harvard.edu. Mailing address for Masato Hirata: Molecular and Cellular Biochemistry, Faculty of Dental Science, Kyushu University, Fukuoka 812-8582, Japan. Phone: 81-92-642-6317. Fax: 81-92-642-6322. E-mail: hirata1@dent.kyushu-u.ac.jp.

▽ Published ahead of print on 19 January 2010.

cell motility and cytokinesis but also in endocytic processes, although the necessity and role in endocytosis in higher eukaryotic cells remain ambiguous (12, 34, 35, 55). The WASP homology 2 (WH2) domain is known as an actin-binding motif found in regulators of the actin cytoskeleton, including Wiskott-Aldrich syndrome protein (WASP), Scar/WASP-family verprolin-homologous protein (WAVE), verprolin/WASP-interacting protein (WIP), missing in metastasis (MIM), and β-thymosins (52). Some proteins with WH2 domains, such as β-thymosin, prevent actin filament assembly by sequestering actin monomers, while others, such as N-WASP and the *Drosophila* protein Ciboulot participate in barbed-end actin assembly (52). Recently, the structural basis for these opposite functions of WH2 domains was demonstrated; the interaction of the C-terminal region of β-thymosin/WH2 domain with the pointed end of the actin monomer accounts for the switch in function from inhibition to promotion of actin assembly (26). WH2 domains exist in almost 20 proteins, whose functions remain to be clarified.

In the present study, we isolated a new multimodular protein (termed PXK), conserved in multicellular organisms including humans through flies, which possesses a PX domain, a protein kinase-like domain, and a WH2 domain. We show that the PX and WH2 domains function as PtdIns(3)P and actin-binding domains, respectively. PXK expression in COS cells accelerated ligand-induced EGFR endocytosis and degradation that was dependent on a functional PX domain but independent of the WH2 domain. PXK also enhanced ubiquitination of EGFR induced by EGF stimulation in these cells. Based on these results, we propose that PXK is a functional sorting nexin that may play an additional role in cellular function via its interaction with the actin cytoskeleton.

MATERIALS AND METHODS

Materials. MG-132 (carbobenzoxy-L-leucyl-L-leucyl-L-leucinal) was obtained from EMD Chemicals (San Diego, CA). Bafilomycin A1 and cycloheximide (CHX) were from Wako Pure Chemical Industries (Osaka, Japan). Human recombinant EGF was from Sigma-Aldrich (St. Louis, MO). Antibodies used in this study were as follows: antihemagglutinin (anti-HA) antibody (HA11; Babco, Richmond, CA); anti-FLAG (M2), anti-pan-cadherin, and anti-β-actin antibodies (Sigma-Aldrich, St. Louis, MO); anti-EGFR and anti-glutathione *S*-transferase (anti-GST) antibodies (Santa Cruz Biotechnology, Santa Cruz, CA); anti-transferrin receptor and anti-EEA1 (early endosomal antigen 1) (BD Biosciences, San Jose, CA); Alexa Fluor 488–anti-mouse, Alexa Fluor 594–anti-rabbit, and Alexa Fluor 488–anti-rabbit antibodies (Invitrogen, Carlsbad, CA); and Cy3–anti-mouse antibody (Jackson Immuno Research Laboratories, West Grove, PA). Hoechst 33258 was from Dojindo Laboratories (Kumamoto, Japan).

Molecular cloning of human *PXK*, preparation of expression constructs, and site-directed mutagenesis. HEP11429 (GenBank Accession number AK000342) is a 2,046-bp human cDNA clone which encodes a PX domain-containing protein and lacks an in-frame termination codon but instead contains a poly(A) sequence at its 3′ end. Searching for expressed sequence tag (EST) clones corresponding to the 3′ end of the gene in human EST databases using the ENSEMBL database revealed several independent human EST clones which almost completely overlapped with the 3′ end of HEP11429, and all EST sequences were mapped to human chromosome 3. Alignment of the sequences of EST clones (GenBank accession numbers BG193644, AA456876, and BG573647) and HEP11429 revealed two missing nucleotides in the 3′ end of HEP11429 prior to the poly(A) sequence, and filling the gaps resulted in appearance of an in-frame translation termination codon immediately following the first missing nucleotide. The resulting 2,048-bp open reading frame of *PXK* was amplified by nested PCR employing *Pfu* Turbo DNA polymerase (Agilent, Santa Clara, CA) using human brain cDNAs as the template. Two different pairs of oligonucleotide primers, whose sequences corresponded to outside or both ends of the open reading frame of the assembled *PXK* sequence, were used for PCR and their sequences are as follows; 5′-TTCCTACCTCGCGTCCCTAG-3′ (sense for the first PCR), 5′-TCCCAGGAAGAGGGTAGTTTGG-3′ (antisense for the first PCR), 5′-GGCGTCCCGGGATGGCCTTCATGGAGAAG-3′ (sense for the second PCR), and 5′-GGAAGCTTCAGCCGATCTTCGGAGC-3′ (antisense for the second PCR). The sequence of the PCR product completely matched that obtained as described above. All expression constructs for PXK were generated by PCR and subcloned into the corresponding vectors. The full-length PCR products or deletion mutants (ΔC [residues 1 to 447], NT [1 to 250], CT [251 to 578], and WH2 [531 to 578]) of PXK were subcloned into pEBG (kindly provided by B. E. Turk, Yale University School of Medicine, New Haven, CT) or pcDNA3-FLAG (provided by B. D. Manning, Harvard University, Boston, MA) vector for expressing GST- or FLAG-tagged proteins in mammalian cells, respectively. The PX domain cDNA (residues 12 to 135) generated by PCR was subcloned into pEGFP-N1 or pEYFP-N1 (Clontech, Mountain View, CA) to express PXK as a fusion to the N terminus of enhanced green fluorescent protein (EGFP) or enhanced yellow fluorescent protein (EYFP), respectively. Retroviral expression vectors for expressing HA-tagged wild-type or mutant PXK were also generated by subcloning cDNA into pBabe-HA-puro vector (provided by J. A. Engelman, Harvard University, Boston, MA). The bacterial vector expressing the PX domain of PXK was also generated by subcloning the corresponding cDNA into pGEX-4T3 (GE Healthcare, Uppsala, Sweden). Human SNX27 was also cloned by PCR using the same cDNAs to amplify PXK and subcloned into pEGFP-N1 vector. The constructs to express GST-fused proteins of the PX domain of $p40^{phox}$ (GST-p40 ^{phox} PX) and EGFP-FYVE3 have been described previously (36). All PXK mutants carrying one or two substitutions of amino acid residues were produced using QuikChange site-directed mutagenesis (Stratagene, La Jolla, CA). All constructs were fully sequenced to verify their integrity at the Beth Israel Deaconess Medical Center DNA Sequencing Core Facility. More details of all constructs are available on request.

Antiserum production. Two rabbit polyclonal anti-PXK antisera were raised against a mixture of keyhole limpet hemocyanin-linked peptides corresponding to residues 477 to 490 (CEHSAKYSNSNNSAG; the initial C was included to conjugate keyhole limpet hemocyanin) and residues 560 to 578 (QKGTLRKA KTCDHSAPKIG) of human PXK. PolyQuick antisera were produced and designated 2963-1 and 2963-2, respectively, by Zymed Laboratories (South San Francisco, CA), and the latter serum was used to detect endogenous PXK in the experiments.

Cell culture, transient transfection, and retroviral infection to establish stable cell lines. COS7 and MDCK cells were purchased from the American Type Culture Collection (ATCC), and HaCaT, a human keratinocyte cell line, was a generous gift from H. Morita (Kyushu University, Japan). All cells were maintained in Dulbecco's modified Eagle's medium (DMEM) supplemented with 10% fetal bovine serum (FBS). Transient-transfection experiments were carried out with Lipofectamine Plus reagents (Invitrogen) according to the manufacturer's instructions. COS7 cells were infected with retroviral vectors as described previously (32), and stable populations were obtained by selection with 8 μg/ml puromycin (Sigma-Aldrich).

RNAi. HaCaT cells were transfected with synthetic small interfering RNA (siRNA) (50 nM duplex; Validated Stealth RNAi DuoPak) specific for human *PXK* (Invitrogen) using HilyMax (Dojindo Laboratories, Kumamoto, Japan), according to the manufacturer's instructions. Two days later, the cells were split into a 12- or 6-well plate, followed by repeated transfection with siRNA. Twenty-four hours after the second transfection, the cells were subjected to EGFR degradation or internalization assays. Scrambled Stealth RNA interference-(RNAi) duplex (stealth RNAi negative control; Invitrogen) was used as the negative control. In initial experiments, we tested three different siRNAs, two from the RNAi DuoPak kit (catalog number 45-3178) and one designed by ourselves. Each of them was designed for different sites of the PXK gene but provided similar results regarding silencing of the PXK gene and EGFR degradation. The target sequence of the RNAi designed by ourselves was 5′-GTTTA AGATCCCTACAAAG-3′. Total RNA was prepared from the cells (RNeasy minikit; Qiagen) after transfection and used as a template to prepare cDNA (High Capacity cDNA Archive Kit; AP Bio) for PCR to confirm silencing of *PXK*. The following primers were used for PCR: F1, 5′-GCAAGGTGCTGCT GGACGACAC-3′; F2, 5′-AGCCAAAGTGGGAGGTGGTGGAAC-3′; R1, 5′-ACTTGTCTGGGCCAAGGTCAGC-3′; and R2, TCAAGGTCCAGCAGC-CGGCAAG-3′. PCR was performed with F1/R1, F1/R2, and F2/R2 primer sets to detect several splice variants of *PXK* (45), and the reaction with each combination of primers gave a single band.

Tissue distribution. Organs isolated from euthanized adult female rats, were homogenized with a Polytron instrument (Kinematica, Luzerne, Switzerland) in ice-cold buffer containing 50 mM HEPES-NaOH (pH 7.4), 150 mM NaCl, 1 mM EDTA, and protease inhibitor cocktail (10 μg/ml leupeptin, 10 μg/ml pepstatin,

10 μg/ml aprotinin, and 10 μg/ml *p*-amidinophenyl methanesulfonyl fluoride hydrochloride), followed by treatment with 1% Triton X-100 for 30 min and centrifugation for 30 min at 16,000 × *g*. The protein concentration in the lysate was determined with the Protein Assay Rapid Kit (Wako Pure Chemical Industries, Osaka, Japan). Twenty micrograms of total protein from each organ was subjected to Western blotting. The experiment was approved by the Animal Care Committee of Kyushu University, following the guidelines of the Japanese Council on Animal Care.

Western blotting. Protein samples were separated by 8% or 10% sodium dodecyl sulfate (SDS)-polyacrylamide gel electrophoresis (PAGE) and then transferred to polyvinylidene fluoride membranes (Millipore, Billerica, MA). Following blocking, the membrane was blotted with the appropriate antibody, and subsequently, horseradish peroxidase-conjugated anti-rabbit or anti-mouse IgG (GE Healthcare) was applied, followed by detection of chemiluminescent signals by exposing the membrane to a film or using an LAS-3000 mini gel documentation system (Fujifilm, Tokyo, Japan). Digital images were analyzed with NIH image software (http://rsb.info.nih.gov/nih-image/) to measure the density of each band without a saturated signal.

Northern blotting. MTN Blot Human 12-lane, a membrane containing mRNA [2 μg poly(A) in each lane], was obtained from Clontech and probed with 662-bp EcoRI-digested fragments of human *PXK* cDNA radiolabeled with ^{32}P using the Rediprime II DNA labeling system (GE Healthcare) in ExpressHyb hybridization solution (Clontech) following the manufacturer's instructions.

Preparation of recombinant proteins. GST-tagged recombinant proteins were expressed using a bacterial expression system and purified with glutathione-Sepharose 4B (GE Healthcare) as described by the manufacturer.

Protein-lipid overlay assay. A protein-lipid overlay assay was performed using GST fusion proteins exactly as described previously (36).

Immunocytochemistry and fluorescence microscopy. All cells for immunofluorescence were grown on 15-mm round coverslips, transiently transfected in a 12-well plate, and observed at 24 h after transfection. To test the effect of PXK expression on EGFR trafficking, COS7 cells transfected with FLAG-PXK constructs were serum starved for 12 h. Thirty minutes before stimulation, the medium was replaced with serum-free DMEM containing 20 μg/ml CHX with or without MG-132 or bafilomycin A1, and the cells were then stimulated with 100 nM EGF in the preincubation medium for 15 min at 37°C, followed by washing and fixation for immunofluorescence. Cells for staining with an antibody against EEA1, transferrin receptor (TfR), or lysosome-associated membrane protein 2 (LAMP-2) were fixed at 24 h after transfection to express PXK. All fixation was performed by washing once with phosphate-buffered saline (PBS) and then incubating in 3.7% paraformaldehyde in PBS (pH 7.4) at 4°C for 30 min. After fixation, the cells were permeabilized with 0.2% Triton X-100 and then blocked with 1% bovine serum albumin, followed by staining. Anti-EGFR antibody (2 μg/ml), anti-FLAG antibody (1 μg/ml), anti-EEA1 antibody (0.5 μg/ml), anti-TfR (4 μg/ml), or anti-LAMP-2 (4 μg/ml) in PBS containing 1% bovine serum albumin was applied for 1 h at room temperature or overnight at 4°C to stain the appropriate molecule. Fluorescent dye-conjugated anti-rabbit or anti-mouse secondary antibody precleared by centrifugation at 16,000 × *g* for 30 min was used at 0.5 μg/ml in PBS containing 1% bovine serum albumin for 2 h at room temperature. In some experiments, the cells were counterstained with Hoechst (5 μg/ml in PBS) for 5 min after secondary antibody incubation. Extensive washing with PBS was performed after each step and before mounting on slides with Permafluor (Beckman Coulter, Fullerton, CA). Images of COS7 cells coexpressing EYFP-PXK/enhanced cyan fluorescent protein (ECFP) and cells expressing EGFP-PXK mutants (R54Q, R55Q, and P74A) were obtained by epifluorescence using a Nikon Diaphot 300 and a Photometrics Sensys charge-coupled device (CCD) (Photometrics, Tucson, AZ) camera with or without 30 min of treatment with 100 nM wortmannin. Confocal imaging was performed on an LSM510 Meta instrument (Carl Zeiss).

Actin binding assay. The actin binding assay was performed as described previously (14), with minor modifications. Briefly, transiently transfected cells expressing GST-PXK or mutants were lysed by rotating in lysis buffer (5 mM Tris-HCl [pH 7.5], 1 mM dithiothreitol, 0.2 mM ATP, 0.1 mM $CaCl_2$, 2 mM $MgCl_2$, 0.1 M KCl) containing 1% Triton X-100 and protease inhibitor cocktail, after washing with ice-cold PBS, at 4°C for 1 h. After removal of insoluble materials by centrifugation, the supernatant was incubated with glutathione beads for 2 h at 4°C. After washing the beads were washed five times with lysis buffer containing 0.2% Triton X-100, they were resuspended in 1× sample buffer and then subjected to 10% SDS-PAGE followed by immunoblotting with anti-β-actin antibody.

Receptor internalization assay. Receptor internalization was analyzed by detecting the remaining cell surface receptors by using a cell surface biotinylation technique. The cells were cultured to 70 to 80% confluence in a six-well plate and then serum starved for 12 h, followed by stimulation with EGF for the indicated time. Stimulated cells were briefly washed with ice-cold PBS containing 0.9 mM $CaCl_2$ and 0.33 mM $MgCl_2$ [PBS(+)], followed by incubation in 1 ml sulfosuccinimidyl-6-(biotin-amido) hexanoate (sulfo-NHS-LC-biotin; 1 mg/ml; Pierce, Rockford, IL) in PBS(+) for 30 min at 4°C in the dark with gentle agitation. Following incubation, unreacted biotin reagent was removed by washing with ice-cold PBS(+) and then quenched by two treatments with 0.1 M glycine in PBS for 5 min. The cells were lysed in radioimmunoprecipitation assay (RIPA) buffer (50 mM Tris-HCl [pH 7.5], 150 mM NaCl, 5 mM EDTA, 5 mM EGTA, 1% Triton X-100, 0.5% Na-deoxycholate, 0.1% SDS, 50 mM NaF, 10 mM $Na_4P_2O_7$, 1 mM dithiothreitol, 1 mM Na_3VO_4, and protease inhibitor cocktail). Biotinylated proteins in the lysates were isolated using streptavidin-coated beads. The amounts of remaining receptor on the cell surface isolated with streptavidin beads were determined by immunoblotting.

Assay of transferrin uptake and recycling. The uptake of biotinylated transferrin (Tf) was assayed according to a method described previously that employed radiolabeled Tf (31). Briefly, cells grown in a 12-well plate were incubated with 10 μg/ml of biotinylated Tf in serum-free DMEM for the indicated time. After washing once with an acid solution (0.2 N acetic acid and 0.2 M NaCl) for 2 min and extensive washing with ice-cold PBS, the cells were fixed with 3.7% paraformaldehyde in PBS, followed by permeabilization with 0.2% Triton X-100 in PBS. After blocking with 1% bovine serum albumin in PBS, the cells were incubated with streptavidin-conjugated alkaline phosphatase. The amount of incorporated biotinylated Tf was then detected using the appropriate soluble substrate. To measure Tf recycling, cells incubated with biotinylated Tf for 60 min as described above were washed once with ice-cold PBS. The cells were further incubated with 500 μg/ml of nonlabeled human holo-Tf for 5 or 30 min. After washing with an acid solution, the amount of remaining biotinylated Tf was measured as described above.

Ligand-induced receptor degradation assay. Cells were cultured to 70 to 80% confluence in a 12-well plate and serum starved for 12 h in serum-free DMEM. The medium was replaced with 20 μg/ml CHX in serum-free DMEM 30 min prior to stimulation with EGF in serum-free DMEM containing CHX. After incubation at 37°C in a CO_2 incubator for the indicated time, the cells were washed with ice-cold PBS and lysed in sample buffer, followed by boiling for 15 min. About 15% of total cell lysates was subjected to SDS-PAGE and Western blotting. MG-132 (10 μM) or bafilomycin A1 (0.25 μM) was also added when cells were incubated in CHX.

Assay of EGFR ubiquitination. Cells grown to 70 to 80% confluence in a six-well plate were serum starved for 12 h in serum-free DMEM, followed by stimulation with 100 nM EGF for the indicated time. The cells were then washed with ice-cold PBS and lysed in RIPA buffer. The lysate was first incubated with 2 μg of anti-EGFR antibody, and the immunocomplex was precipitated using protein G-Sepharose. The immunoprecipitate was subjected to Western blotting to detect ubiquitinated EGFR using antiubiquitin antibody. In some experiments, bafilomycin A1 (0.25 μM) was added to inhibit lysosomal degradation 30 min before EGF stimulation.

Statistics. All statistical comparisons were evaluated on a Macintosh computer with GraphPad Prism 4 (GraphPad Software, San Diego, CA). All values are the means ± standard errors (SEs).

RESULTS

Identification of PXK, a novel molecule comprising PX and WH2 domains and a protein kinase-like region. We searched sequence databases for novel proteins harboring the PX domain and identified a series of overlapping human expressed sequence tag (EST) clones, all mapping to a common region of human chromosome 3 (3p14.3), that assembled into a 2,048-bp open reading frame that encoded a 578-residue protein containing an N-terminal PX domain, a central protein kinase-like domain and a C-terminal WH2 domain. The mRNA is encoded by 18 exons, and the gene is now denoted *PXK* (PX domain-containing serine/threonine kinase) in Entrezgene (GeneID 54899) on the NCBI website. The gene product is highly conserved among species from flies through humans but not in nematodes or yeast.

Tissue distribution of PXK. The expression of *PXK* mRNA in human tissues was examined by Northern blotting. As shown in Fig. 1A, the major 3-kb transcript was present almost ubiq-

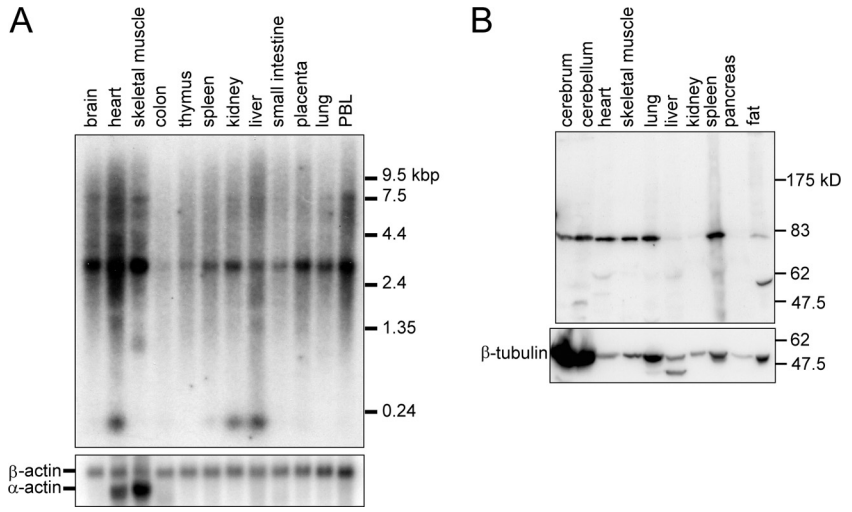

FIG. 1. Tissue expression of PXK. (A) Tissue distribution of human *PXK* mRNA. The blot membrane containing 2 μg human mRNA in each lane was probed with a 662-bp fragment of EcoRI-digested *PXK* cDNA and reprobed with the control probe for β-actin. The sizes of the markers are shown on the right. (B) Tissue expression of PXK protein in rats. Rat tissue extract (40 μg protein) was subjected to immunoblot analysis of PXK by probing with rabbit anti-human PXK antiserum. A blot of β-tubulin as a loading control is also shown. The molecular sizes of the markers are shown at the right.

uitously among the human tissues tested, with the highest expression in the brain, heart, skeletal muscle, placenta, and peripheral blood lymphocytes (PBL). Protein expression levels in rat tissues were also examined by immunoblotting with rabbit anti-PXK antiserum (Fig. 1B). The specificity of the antiserum was confirmed by immunoblotting with the cell lysate of COS7 cells transiently transfected to express FLAG-tagged recombinant human PXK. A single band with a predicted molecular mass of 75-kDa, comigrated with FLAG-PXK (data not shown) and was present almost ubiquitously among the tissues tested, with an additional band of smaller molecular size in white fat tissue.

The PX domain of PXK interacts with PtdIns(3)P and localizes to endomembrane structures. Sequence alignment of PX domains revealed that the PX domain of PXK has conserved basic and aromatic amino acid residues in the β3 strand which are responsible for phosphoinositide recognition of PX domains (Fig. 2A) (6). The conserved polyproline region in the variable loop between the α1 and α2 helices also exists in the PX domain of PXK (Fig. 2A). To test if the PX domain of PXK interacts with phosphoinositide, we performed the protein-lipid overlay assay (36). The PX domain of PXK showed specific interaction with PtdIns(3)P (Fig. 2B). Consistent with the binding specificity, we found that PXK colocalizes mainly with EEA1, a marker protein for early endosomes (Fig. 2C), where PtdIns(3)P is most abundant in mammalian cells (11). In addition, we also observed colocalization of PXK with TfR and LAMP-2, marker proteins for recycling endosomes and late endosomes/lysosomes, respectively (Fig. 2C). We estimated the fractions of PXK overlapping with the markers and found that 62% ± 6.2%, 38% ± 11.2%, and 12% ± 6.4% of the PXK signals overlapped with EEA1, TfR, and LAMP-2, respectively. During the experiment, we noticed that there were some differences in the subcellular localization of PXK depending on the tags fused to the protein. PXK tagged with FLAG at the N terminus and with EGFP at the C terminus showed comparable subcellular localization, while the protein with N-terminally fused EGFP showed less clustered localization. Thus, we used FLAG-tagged or C-terminally EGFP-tagged PXK throughout the study.

The contribution of PtdIns(3)P binding of the PX domain to endosomal localization of PXK was confirmed by wortmannin sensitivity and mutational analysis. Endosomal localization of PXK-EYFP was disrupted by treating the cells with wortmannin, a phosphoinositide 3-kinase (PI3K) inhibitor, while the vehicle, dimethyl sulfoxide (DMSO), had little effect on the localization of PXK-EYFP (Fig. 2D). Site-directed mutagenesis of the conserved basic residues (R54Q or R55Q) which are involved in PX domain binding to phosphate groups of phosphoinositides (6) completely abolished endosomal localization of PXK-EGFP (Fig. 2E), indicating that the basic residues are required primarily for endosomal localization. The isolated PX domain of PXK alone, expressed as an EGFP-fused protein in COS7 cells, showed a diffuse distribution throughout the cytoplasm (data not shown), indicating that this domain, as an isolated protein, has insufficient affinity to bind to endosomes. Since the conserved proline-rich regions of other PX domains have been shown to be functional SH3 domain ligands (1, 4) and many SH3 proteins show endosomal localization (46), we then examined the effect of substituting proline for one of the alanine residues in the conserved PXXP motif (P74A) on subcellular localization of PXK. The P74A mutant of PXK-EGFP showed localization to the perinuclear region, albeit to a lesser extent than the wild type, indicating that the endosomal localization of PXK is not primarily mediated by SH3 proteins residing in endosomes.

The WH2 domain of PXK is a functional actin-binding domain. The basic amino acid residues directly contributing to interaction of the WH2 domains with monomeric actin are conserved in the WH2 domain of PXK (Fig. 3A, indicated by asterisks) (52). To determine whether the WH2 domain of PXK has the ability to interact with actin, we performed a pulldown assay with wild-type or deletion mutants of GST-

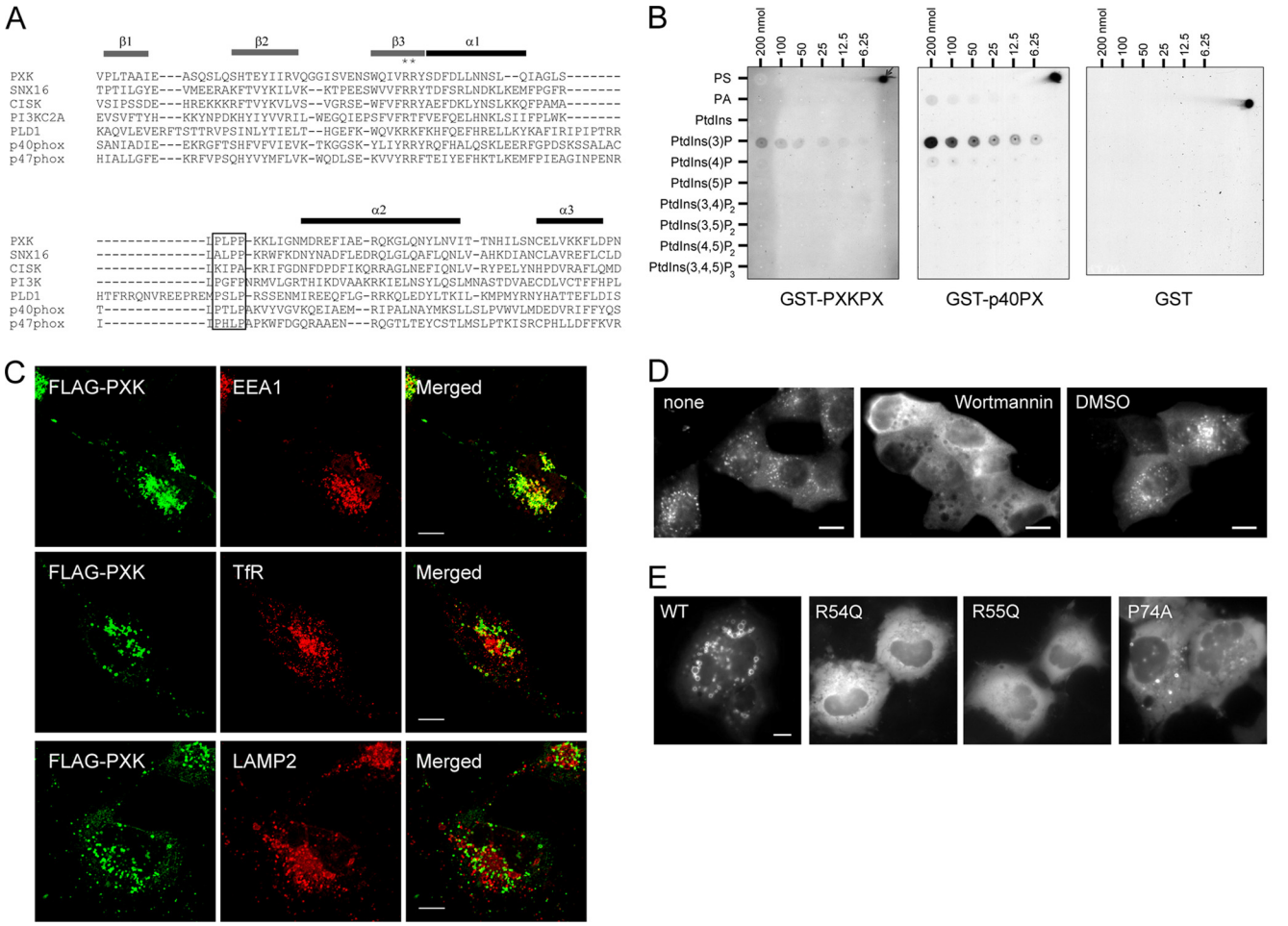

FIG. 2. Endosomal localization of PXK depends on phosphoinositide binding of the PX domain. (A) Sequence alignment of several PX domains. Sequences were aligned using ClustalW and a Gonnet-weight matrix with a gap-opening penalty of 5 and extension penalty of 0.05 for multiple alignments, with some modification by hand to adjust the positions of proline-rich motifs. Highly conserved Arg residues are indicated by asterisks, and proline-rich regions are boxed. Secondary structure elements are aligned according to the PX domain of $p40^{phox}$ and are shown at the top. All PX domains in the alignment are from human homologs, and the GenBank accession numbers and corresponding amino acids are as follows: PXK, NP060241, 18 to 122; SNX16, NP690049, 109 to 214; CISK (cytokine-independent survival kinase), NP037389, 16 to 120; PI3K-C2α, NP002636, 1426 to 1534; PLD1, NP002653, 82 to 206; $p40^{phox}$, NP038202, 23 to 136; and $p47^{phox}$, NP000256, 8 to 121. (B) Phospholipid-binding property of the PX domain from human PXK. The ability of GST fusion proteins to bind a variety of phospholipids was analyzed using a protein-lipid overlay assay. Serial dilutions of the indicated phospholipids were spotted onto nitrocellulose membranes, which were then probed with GST fusion proteins, followed by detection using anti-GST antibody. Each GST fusion protein (1 pmol) was also spotted in the upper right corner of the membrane. PS, phosphatidylserine; PA, phosphatidic acid. (C) COS7 cells cultured on coverslips were transfected to express FLAG-PXK and visualized in green for FLAG-PXK and red for EEA1, TfR, or LAMP-2 by indirect immunofluorescence using a combination of rabbit antibody against FLAG and Alexa 594-conjugated rabbit IgG and mouse antibodies against EEA1, TfR, or LAMP-2 and Cy3-conjugated mouse IgG, respectively. The yellowish staining in the merged picture indicates colocalization with FLAG-PXK. For quantification, the number of the yellowish punctates and the total number of FLAG-PXK-positive, greenish punctuates were counted manually and the ratio was calculated. More than 10 cells were counted for each experiment. Scale bars, 10 μm. (D) Madin-Darby canine kidney (MDCK) cells cultured on coverslips were transfected to express PXK-EYFP, followed by treatment with 100 nM wortmannin or the vehicle, dimethyl sulfoxide (DMSO) for 20 min. Scale bars, 10 μm. (E) Subcellular localization of PXK-EGFP carrying point mutations in the PX domain in COS7 cells. WT, wild type. Scale bars, 10 μm.

tagged PXK expressed in COS7 cells. As shown in Fig. 3B, endogenous actin was coprecipitated with GST-PXK constructs which carry intact WH2 domains (full, CT, and WH2) but not with mutants in which the WH2 domain was deleted (ΔC and NT). The introduction of point mutations in residues predicted to be involved in actin binding, R565G/K566Q (PXK-RGKQ), also abolished actin binding of PXK (Fig. 3B).

Characterization of the protein kinase-like domain of PXK. Although PXK has a domain with homology to protein-Ser/Thr kinases, residues highly conserved in kinases are not conserved in this domain of PXK. One substitution is the lysine residue interacting with the α- and β-phosphates of ATP to anchor and orient ATP in the Val-Ala-Ile-Lys (VAIK) motif from subdomain II. The His-Arg-Asp (HRD) motif in subdomain VIb, in which the aspartic acid is the catalytic residue functioning as a base acceptor to achieve proton transfer, is replaced by His-Leu-His (HLH). The Asp-Phe-Gly (DFG) motif in subdomain VIIin with which magnesium-binding as-

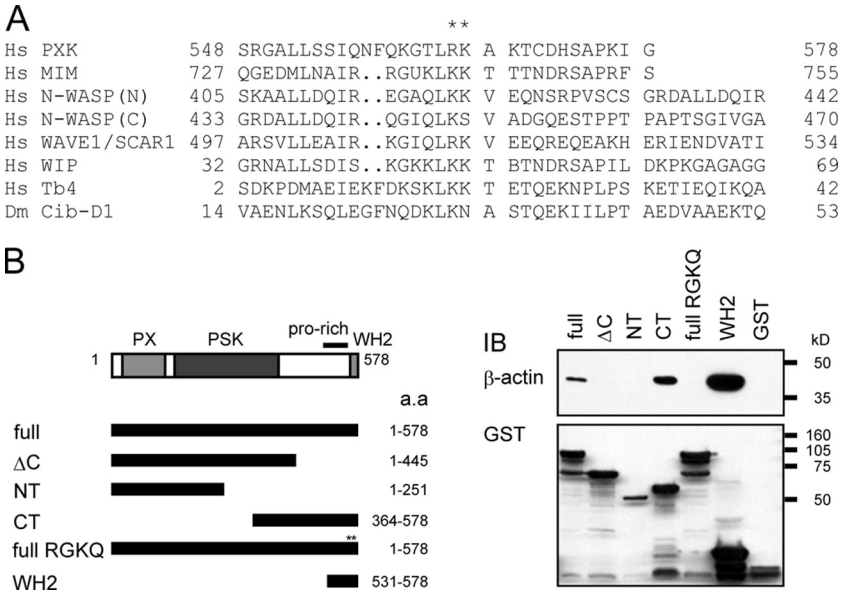

FIG. 3. The WH2 domain of PXK is a functional actin-binding domain. (A) Sequence alignment of WH2 motifs. Basic residues with asterisks are highly conserved. GenBank accession numbers of parental proteins are as follows: human PXK, NP060241; human MIM, NP055566; human N-WASP, NP003932; human WAVE1/Scar1, NP003922; human WIP, NP003378; human thymosin β4, NP066932; and *Drosophila* Ciboulot, NP726908. (B) Actin binding assay. Wild-type or mutant PXK fused to GST was expressed in COS7 cells and collected using glutathione beads from cell lysates. The intrinsic actin copurified with GST-PXK mutants was analyzed with anti-β-actin antibody. An immunoblot (IB) with anti-GST antibody is also shown. A schematic representation of PXK mutants is shown on the left. PX, PX domain; PSK, pseudo-kinase (kinase-like) domain; Pro-rich, proline-rich region before the WH2 domain (not the proline-rich region in the PX domain; see also Fig. 2A); WH2, WH2 domain.

partic acid coordinates β- and γ-phosphates of ATP, is replaced by Asp-Leu-Glu (DLE). In addition, neither the glycine-rich loop in subdomain I nor the corresponding glutamate residue in subdomain III, which helps stabilize the interactions between lysine from subdomain I and α- and β-phosphates of ATP, exists (21, 56). Therefore, we were unable to detect autophosphorylation of PXK or phosphorylation of commonly used protein kinase substrates such as myelin basic protein or histone H2B (not shown). Zou et al. showed that a similar kinase domain in Slob exhibited increased catalytic activity after being phosphorylated by protein kinase A (75), so we further examined the kinase activity of PXK after treatment with protein kinase A or protein kinase C, but we detected no intrinsic activity (not shown). These results suggest that PXK may be a "dead" kinase, analogous to STRAD, ErbB3, and KSR (5).

PXK promotes ligand-induced internalization of EGFR. We first investigated the possibility that PXK acts as a sorting nexin. The effect of PXK expression on ligand-induced EGFR endocytosis was examined by a cell surface biotinylation assay. We generated cell lines stably expressing HA-tagged PXK. COS7 cells stably expressing HA or HA-PXK were stimulated with EGF at 10 nM for 5 min, followed by biotinylation of proteins remaining on the cell surface, including EGFR. EGF induced a reduction of the amount of cell surface EGFR in cells expressing HA-PXK but had little effect on control cells expressing HA alone (Fig. 4A and B), indicating that PXK accelerates the ligand-induced internalization of EGFR. On the other hand, the amount of cadherin on the cell surface was unaffected by HA-PXK expression (Fig. 4A, bottom panel). Stimulation of the cells with a higher concentration of EGF

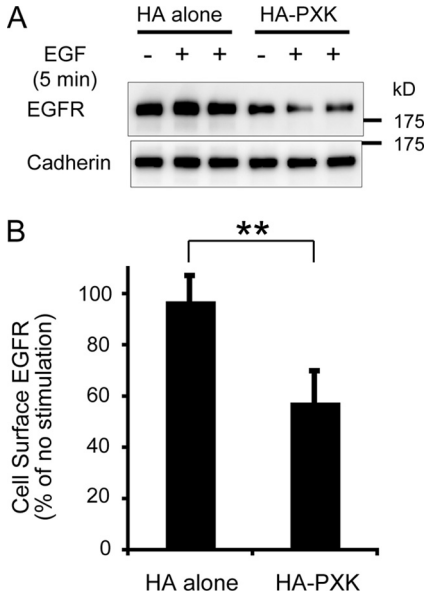

FIG. 4. PXK promotes ligand-induced EGFR internalization. (A) COS7 cells stably expressing HA or HA-PXK were starved for 12 h prior to stimulation with 10 nM EGF for 5 min. After EGF stimulation, cell surface proteins were biotinylated, followed by precipitation using streptavidin beads from the cell lysate and immunoblotting to detect the amounts of EGFR and pan-cadherin. (B) The density of each band, quantified using NIH Image software, is shown after normalization with cadherin. One hundred percent was obtained for each cell with no stimulation. Data are the means ± SEs from three experiments in duplicate. **, statistically different ($P < 0.01$) from the control.

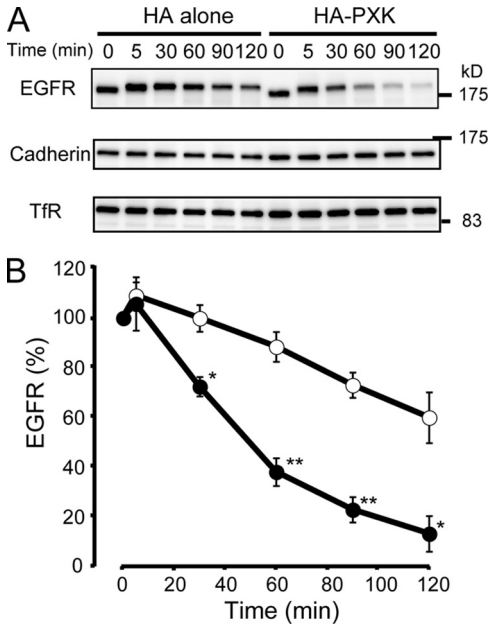

FIG. 5. Effect of PXK expression on ligand-induced EGFR degradation. (A) COS7 cells stably expressing HA alone and HA-PXK were serum starved for 12 h, followed by incubation with 20 μg/ml CHX and 100 nM EGF for the times indicated. Cells were lysed, and EGFR was analyzed by immunoblotting. The same blot was reprobed with anti pan-cadherin and TfR. (B) The density of EGFR, quantified using NIH Image software, was plotted after normalization with cadherin. Open and closed symbols indicate the values obtained with cells expressing HA alone and expressing HA-PXK, respectively. Data are the means ± SEs from three experiments. *, $P < 0.05$; **, $P < 0.01$ (different from cells expressing HA alone).

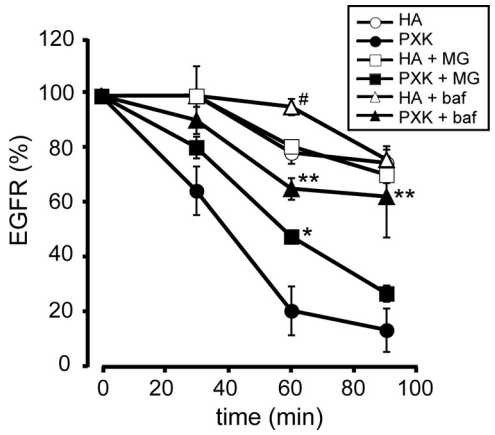

FIG. 6. MG-132 and bafilomycin A1 block EGFR degradation accelerated by PXK. COS7 cells stably expressing HA alone and HA-PXK were starved for 12 h, followed by pretreatment with each inhibitor for 30 min in the presence of CHX. Cells were then stimulated with 100 nM EGF in medium containing inhibitors for the indicated times. The amount of EGFR remaining in cell lysates after EGF stimulation is shown as described for Fig. 5. Data are the means ± SEs from three experiments. #, $P < 0.05$ (different from HA cells [open circle]). *, $P < 0.05$; **, $P < 0.01$ (different from HA-PXK cells [closed circles]).

(100 nM) induced robust internalization of EGFR, thus exhibiting indistinguishable effects in cells expressing HA alone and HA-PXK (not shown).

PXK accelerates ligand-induced EGFR degradation. Whole-cell lysates from cells stimulated with 10 nM EGF for the indicated times were subjected to SDS-PAGE followed by immunoblotting. As shown in Fig. 5, PXK expression resulted in an increased rate of ligand-induced EGFR degradation, while the amount of TfR was unchanged throughout the periods examined.

Effects of proteasomal and lysosomal inhibitors on EGFR degradation in PXK-expressing cells. Next we tested if the inhibitors prevent EGFR from accelerated degradation in PXK-expressing cells (Fig. 6). Cells expressing HA alone (control) or HA-PXK preincubated with protease inhibitors for 30 min were stimulated with EGF for various periods, followed by quantification of EGFR in the lysates. In control cells, ligand-induced EGFR degradation of about 20 and 25% was observed at 60 and 90 min, respectively, which was prevented only by the lysosomal inhibitor (bafilomycin A1) at 60 min but not by the proteasomal inhibitor (MG-132). On the other hand, in PXK-expressing cells, degradation of about 80% and 85% was achieved at 60 and 90 min, respectively, and the acceleration of ligand-induced degradation of EGFR was restored partially by each of the inhibitors but more effectively by bafilomycin A1 than by MG-132 (Fig. 6). The stronger effect of bafilomycin A1 on ligand-induced degradation of EGFR was consistent with previous observations using HER-14 or HeLa cells (2, 64).

PXK modifies EGFR trafficking. The intracellular EGFR signals seen in the perinuclear region in FLAG-PKX-positive cells was not observed when the cells were cultured under serum starvation conditions for 12 h (Fig. 7A, panels 1 and 2). Stimulation with a high concentration of EGF (100 nM) for 5 min led to the appearance of intracellular EGFR signals similarly in both FLAG-PXK-positive and -negative cells (Fig. 7A, panels 3 and 4). Further stimulation with EGF for 30 min led to an increase of EGFR staining in the perinuclear region in control cells, while a decrease was seen in FLAG-PXK-expressing cells (Fig. 7A, panels 5 and 6), consistent with degradation of the EGFR as seen in Western blots (Fig. 5).

The effects of lysosomal and proteasomal inhibitors on EGFR signals were examined. Cells expressing FLAG-PXK were preincubated for 30 min with the lysosomal and proteasomal inhibitors bafilomycin A1 and MG-132, respectively, followed by stimulation with 100 nM EGF for 30 min and visualization for EGFR and FLAG-PXK. Both chemicals prevented the decrease in EGFR staining in FLAG-PXK-positive cells (Fig. 7B, panels 1, 2, 3, and 4), consistent with the results observed in the blot assays (Fig. 6). The less-clustered localization of FLAG-PXK observed in panel 2 of Fig. 7B might be the result of misconfiguration of the lysosomal membrane system caused by the treatment with bafilomycin A1.

The decrease in intracellular EGFR was also observed in cells transfected with the RGKQ mutant of FLAG-PXK (Fig. 8A, panels 1 and 2), suggesting that actin binding of PXK is not required for this effect. On the other hand, FLAG-PXK-R55Q, a PtdIns(3)P binding-deficient mutant, did not decrease EGFR signals (Fig. 8A, panels 3 and 4), thus indicating that PtdIns(3)P binding and/or endosomal localization via binding is indispensable for the effect of PXK on endocytosed EGFR.

Since PtdIns(3)P plays an important role in recruiting molecules involved in trafficking (37, 63), exogenous expression of

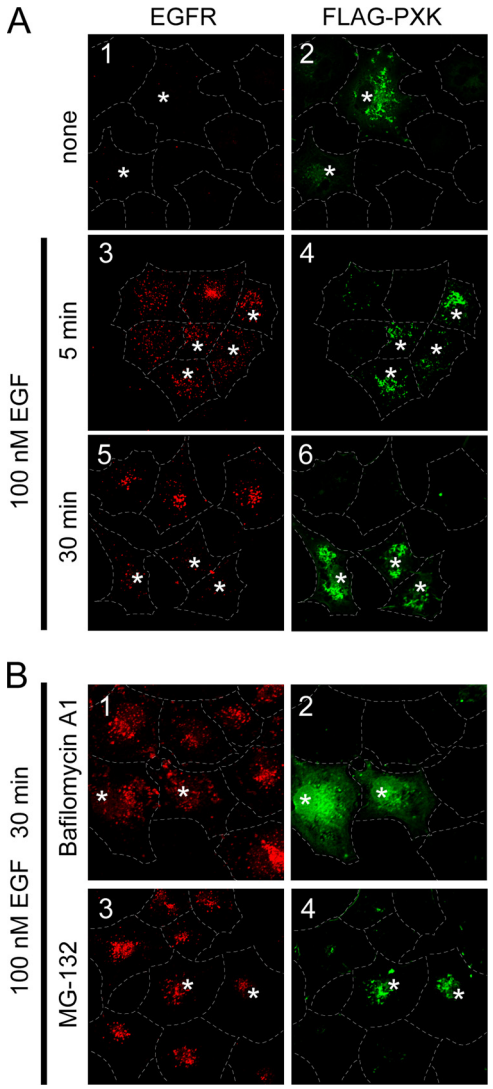

FIG. 7. PXK expression accelerates EGFR degradation. COS7 cells cultured on coverslips were transfected with the gene for FLAG-PXK. Cells showing FLAG fluorescence are indicated by asterisks at the nucleus, and the cellular edges are traced by broken lines. (A) Thirty-six hours after transfection, cells were serum starved for 12 h, followed by preincubation with 20 μg/ml CHX and then left unstimulated (none) or stimulated with 100 nM EGF for 5 or 30 min. Cells were then fixed and treated with mouse anti-FLAG antibody and rabbit anti-EGFR antibody, followed by visualization with Alexa Fluor 488-conjugated anti-mouse antibody (green) and Alexa Fluor 594-conjugated anti-rabbit antibody (red), respectively. (B) Cells were preincubated with 10 μM MG-132 or 0.25 μM bafilomycin A1 in the presence of 20 μg/ml CHX for 30 min and then stimulated with 100 nM EGF for 30 min, followed by treatment as described above. Bars, 10 μm.

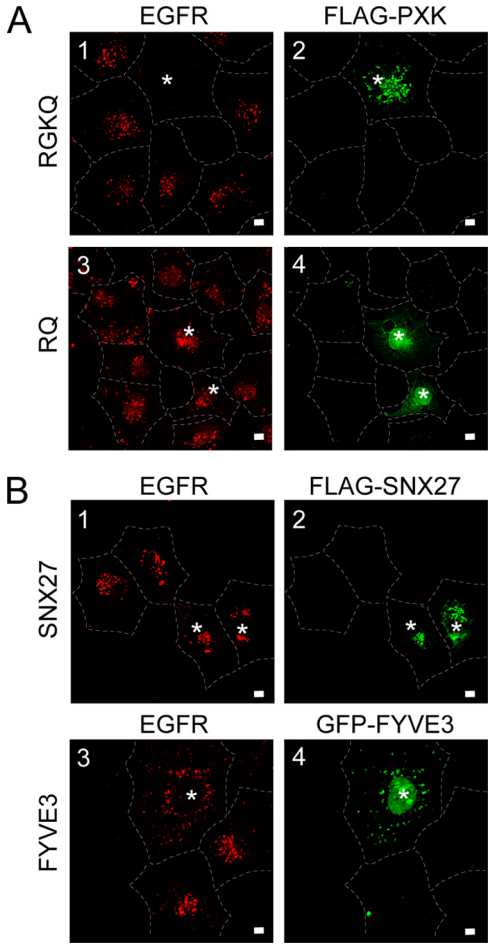

FIG. 8. PXK expression accelerates EGFR degradation. Immunofluorescence analysis was performed as described for Fig. 7. (A) COS7 cells were transfected with genes for FLAG-tagged mutant PXK (RGKQ or RQ as indicated at the left), followed by visualization of EGFR and PXK. (B) COS7 cells were transfected with the gene for FLAG-SNX27 or EGFP-FYVE. Bars, 10 μm.

PtdIns(3)P-binding proteins might affect endogenous events. To exclude this possibility, we examined the effect of the expression of other PtdIns(3)P-binding proteins in these experiments. As shown in Fig. 8B, the effects of the expression of specific PtdIns(3)P-binding proteins on EGFR signals were tested in the same experiments as for PXK, using SNX27 and FYVE3, which are other PX domain proteins (44), and three tandem versions of the FYVE domain from EEA1 (15, 36, 51). Neither SNX27 (Fig. 8B, panels 1 and 2) nor FYVE3 (Fig. 8B, panels 3 and 4) altered EGFR degradation under the same conditions as PXK. These results suggest that the expression of FLAG-PXK results in decreased ligand-induced intracellular accumulation of EGFR by accelerating EGFR degradation.

Depletion of PXK delays both ligand-induced degradation and internalization of EGF receptors. We further examined the effect of the depletion of endogenous PXK protein levels on ligand-induced degradation and internalization of EGFR. In this experiment, we used HaCaT, a human keratinocyte cell line which expresses endogenous PXK and EGFR. The endogenous expression of PXK was successfully depleted using synthetic siRNA duplex (Fig. 9A). These cells were analyzed for EGFR remaining in cell lysates (Fig. 9B) and on cell surfaces (Fig. 9C) after ligand stimulation. Degradation of EGFR was delayed in cells deficient in endogenous PXK: EGFR in mutant cells was slightly degraded after 1 h of stimulation with EGF, while EGFR was degraded by more than 50% during the same period in control cells (Fig. 9B). Degradation proceeded in experimental cells at 2 h after stimulation but was still slower than that in control cells. Quantification of EGFR remaining on the cell sur-

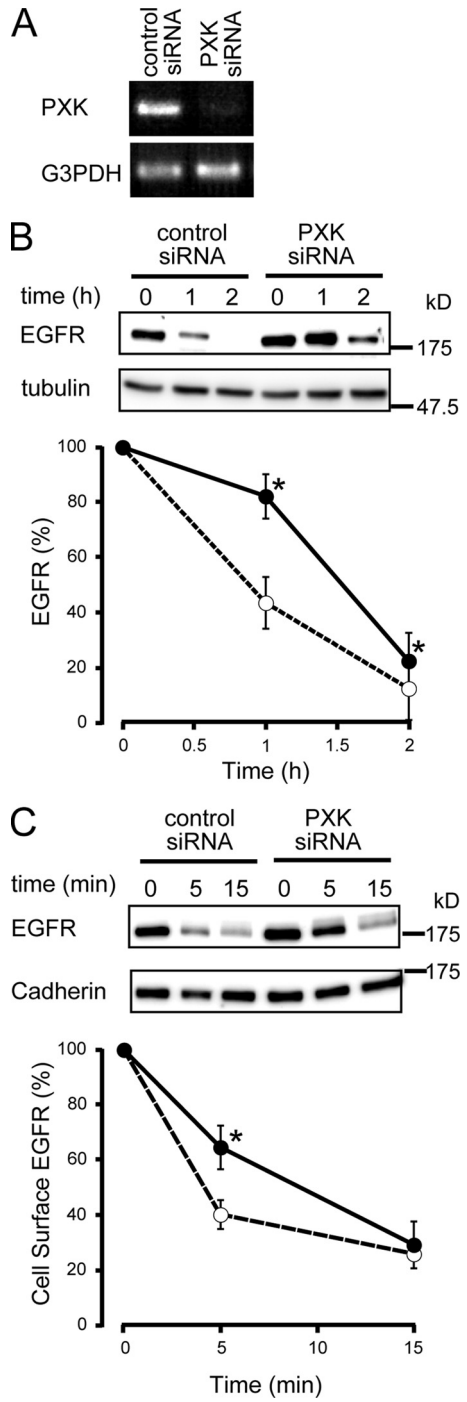

FIG. 9. Effect of endogenous PXK depletion on ligand-induced internalization and degradation of EGFR. Endogenous PXK in HaCaT cells was depleted by transfecting with siRNA. (A) *PXK* silencing was confirmed by reverse transcription-PCR from total RNA of HaCaT cells transfected with siRNA specific against *PXK* or scrambled siRNA duplex as a control. Ethidium bromide staining is shown. (B) EGFR in HaCaT cell lysates stimulated with 200 nM EGF for the indicated times was analyzed as for Fig. 5. Open circles, control; closed circles, PXK-depleted cells. (C) EGFR remaining on the cell surface after 20 nM EGF stimulation for the indicated times was analyzed as for Fig. 4. Open circles, control; closed circles, PXK-depleted cells. Each point is the mean ± SE for three experiments. ⋆, $P < 0.05$, different from control siRNA-treated cells (open circles).

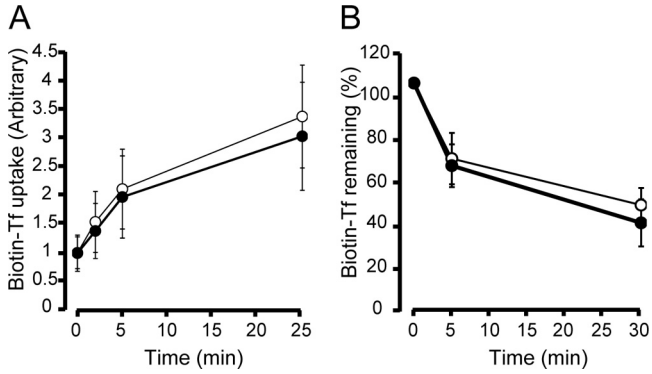

FIG. 10. Effect of PXK expression on uptake and recycling of transferrin. Biotinylated Tf in cells was monitored as an index of the receptors. (A) Control (open circles) or PXK-expressing (closed circles) cells were incubated in the presence of biotinylated Tf (10 μg/ml) for the times indicated. (B) Cells incubated with biotinylated Tf for 60 min were then incubated with 500 μg/ml nonlabeled Tf for 5 or 30 min. After fixation and permeabilization, biotinylated Tf was quantified with streptavidin-conjugated alkaline phosphatase. Each point is the mean ± SE from three experiments.

face revealed that HaCaT cells exhibited faster internalization than the COS7 cells used in the experiments shown in Fig. 4, but the process was delayed by PXK depletion, as shown in Fig. 9C.

Possible sites for PXK to modify EGFR trafficking. To examine the possibility that PXK perturbs global receptor internalization and the whole endosomal network in a nonspecific manner, we tested the effect of PXK expression in COS7 cells on TfR trafficking, which is well known to follow the recycling endosomal system. Biotinylated Tf (10 μg/ml) was incubated with either the control or PXK-expressing cells for up to 25 min for the uptake experiments (Fig. 10A), and for the recycling experiments, the cells were incubated with 10 μg/ml biotinylated Tf for 60 min, followed by incubation with 500 μg/ml nonlabeled holo-Tf for 5 and 30 min (Fig. 10B). Biotinylated Tf inside the cells was assayed by the addition of an enzyme-conjugated streptavidin. As shown in Fig. 10, little difference in either uptake or recycling of biotinylated Tf as a trace of the receptors was observed, indicating the specific role of PXK in perturbation of the EGFR endolysosomal process.

Since ubiquitination of the receptor is a key event in promoting sorting of the receptor to the lysosomal degradation system via incorporation into multivesicular bodies (61), we next examined whether the ubiquitination of EGFR was modified by PXK or not. As shown in Fig. 11A, panel 1, EGFR was ubiquitinated within 5 min in response to 100 nM EGF stimulation, and the level was slightly increased at 15 min, followed by a gradual decrease in the control cells, while PXK-expressing cells showed a robust increase of ubiquitination at 5 min, followed by a gradual decrease. However, the amounts of EGFR in the immunoprecipitates decreased with the time of incubation, especially in the PXK-expressing cells, as shown in panels 1 and 2 of Fig. 11A for the blot and the quantification, respectively. The level of ubiquitination relative to the amounts of the receptor in the immunoprecipitates is depicted in Fig. 11A, panel 3, showing higher ubiquitination of EGFR in PXK-expressing cells. Same experiments were performed in the presence of bafilomycin A1 to inhibit lysosomal degradation of the receptor (Fig. 11B). Under this condition, the

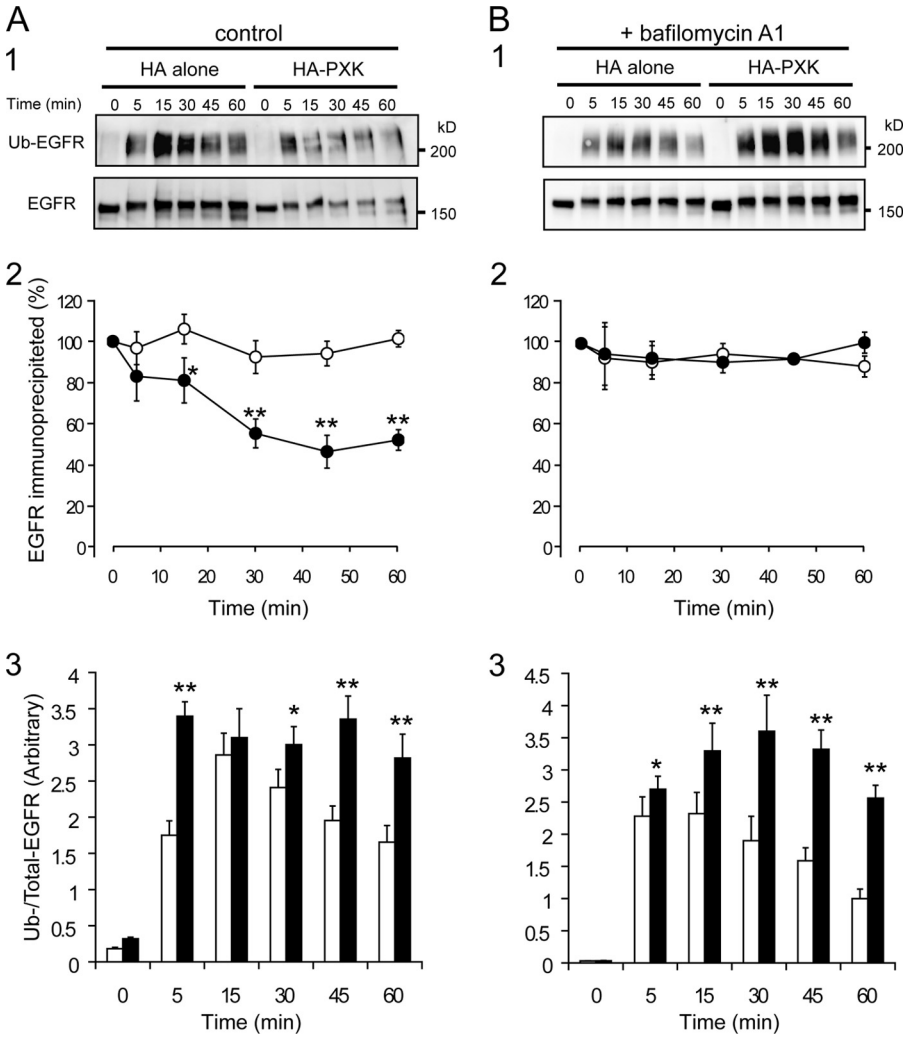

FIG. 11. Effect of PXK expression on ubiquitination of EGFR. Cells expressing either HA alone (open symbols or bars) or HA-PXK (closed symbols or bars) were stimulated with 100 nM EGF for the indicated times. Cell extracts were then immunoprecipitated with 2 μg of anti-EGFR antibody and protein G-Sepharose, followed by Western blotting for ubiquitinated and total EGFR using antiubiquitin and anti-EGFR antibodies, respectively. Panels 1, typical blots; panels 2, density of EGFR quantified by NIH image software; panels 3, ratio of ubiquitination of EGFR. Data are the means ± SEs from three experiments. *, $P < 0.05$; **, $P < 0.01$ (different from cells expressing HA alone). Experiments were performed in the absence (A) or presence (B) of bafilomycin A1.

amounts of EGFR were constant (Fig. 11B, panel 2), and thus the level of ubiquitinated EGFR was apparently higher in PXK-expressing cells (Fig. 11B, panels 1 and 3 for the blot and the quantification, respectively). The PXK effect on the ubiquitination was as expected in the knockdown cells prepared by a siRNA system, but the difference from the control was very small (data not shown). These results indicate that PXK promotes the ubiquitination of EGFR and thus the following endolysosomal trafficking for degradation.

DISCUSSION

In the present study, we isolated the multidomain protein PXK, consisting of a PX domain, a protein kinase-like domain, a proline-rich region, and a WH2 domain, and then analyzed it by biochemical and cell biological characterization. PXK is highly conserved among species from flies through humans but is not present in yeast, and it is expressed ubiquitously in human and rat tissues. PXK is localized mainly at the endosomal membrane, and PtdIns(3)P-specific binding of the PX domain is required for this localization. We present evidence that PXK is involved in ligand-induced internalization and degradation of the EGFR. The intact PX domain is required to modulate EGFR trafficking by PXK, while the actin-binding ability of the WH2 domain is not essential for this function. The results suggest that PXK is a multifunctional protein involved in endocytosis/sorting events, although the function of the actin-binding ability remains to be clarified.

While we were investigating the molecular function of PXK, the *PXK* gene was cloned by two other independent groups. Zou et al. reported that there were five splice variants of the human *PXK* gene with different subcellular localization (75), and Mao et al. showed that PXK, designated MONaKA (modulator of Na,K-ATPase), modulated the activity of the Na,K-

ATPase, as assessed by catalytic activity and functional ion transport activity, by directly interacting with the β-subunit (45). The ubiquitous tissue distribution of PXK, analyzed by Northern blotting and Western blotting in this study, correlated with the results obtained by reverse transcription-PCR analyses in those reports. Although we did not examine the interaction with Na,K-ATPase, PXK might also regulate the trafficking and cell surface expression of the membrane ion pump through a mechanism analogous to that by which PXK modifies EGFR trafficking.

Kinase-like region of PXK. A search for protein domains revealed that PXK contains a putative kinase domain in the middle of the molecule but lacks conserved catalytic residues for known protein kinases, as mentioned by Zou et al. (75). Interestingly, however, the *Drosophila* homolog of PXK (GenBank accession number NP610341), encoded by the CG8726 gene, shows high homology in the putative kinase domain with another *Drosophila* protein, Slob (GenBank accession number NP477349). Slob, identified as a protein interacting with Slowpoke, a calcium-dependent potassium channel (57), was reported to have weak protein kinase activity when activated by protein kinase A, despite lacking the residues conserved in the kinase region in general protein kinases (70). Although the kinase-like domain of PXK was found to be intrinsically inactive, it still might have some physiological functions after modification by or interaction with other factors, such as Slob. There are a number of examples of pseudokinases having critical roles in cellular signaling, including STRAD, KSR, and another PX domain-containing pseudokinase, RPK118 (5). For example, RPK118 has been reported to interact with sphingosine kinase 1 and peroxiredoxin 3, through the kinase-like region, and thus to regulate the cellular localization of these binding partners (25, 42). Indeed, a potential molecule (CG2224) interacts with the *Drosophila* homolog of *PXK* (CG8726) reported in the BioGRID database (http://www.thebiogrid.org/index.php), which was identified by a systemic two-hybrid experiment (16). Thus, the kinase-like domain of PXK might have some role involving participation in protein-protein interaction, as Zou et al. speculated (75).

Subcellular localization of PXK. We showed that PXK was localized mainly to the early endosomes, but some fractions of PXK also localized to both recycling endosomes and late endosomes/lysosomes, in a PI3K-dependent manner since wortmannin abolished the localization. Specific recognition of PtdIns(3)P by the PX domain was indispensable for localization, as point mutations in the essential basic residues abolished endosomal localization. Replacement of the proline residue by alanine (P74A) in the SH3 ligand motif of the PX domain did not abrogate the endosomal localization of PXK, although the mutant showed diminished localization compared to the wild type. The conserved basic residues just following the PXXP motif have been shown to directly contribute to phosphoinositide binding (6). The point mutation of the proline residue (P74A) might affect the basic residues for the interaction indirectly, thus producing diminished localization (Fig. 2E). An *in vitro* lipid binding experiment with the PX domain of PXK showed relatively weak interaction with PtdIns(3)P compared to that with the $p40^{phox}$ PX domain. The isolated PX domain of PXK fused to EGFP did not show endosomal localization, suggesting that other intermolecular interactions might be required for endosomal localization of PXK, in addition to PtdIns(3)P binding of the PX domain. Endosomal targeting of the prototypical sorting nexin, SNX1, requires not only specific PtdIns(3)P binding but also the C-terminal Bin-Amphiphysin-Rvs (BAR) domain (73, 74). Other PX domain-containing proteins, including SNXs and CISK, have been reported to form homo- or hetero-oligomers (50, 66, 73), but we have not obtained evidence of any homo-oligomerization of PXK in coimmunoprecipitation experiments using recombinant protein fused with different tags. Thus, endosomal localization does not require homo-oligomerization of PXK, which is different from the FYVE domain protein or SNXs, which require dimerization (10, 24, 66, 73). On the other hand, a series of PXK mutants carrying a point mutation within the kinase-like domain was constructed for cellular localization, and some mutants showed a diffuse distribution throughout the cytoplasm (H. Takeuchi et al., unpublished observations), supporting the idea that the kinase-like domain contributes to endosomal localization of PXK as a protein-protein interaction domain, as discussed above.

Actin binding of PXK. Dynamic actin cytoskeletal reorganization is important for cell migration, polarity, and membrane trafficking (49). Not only assembling but also disassembling actin molecules have been implicated in endocytosis, membrane fusion, membrane invagination, and exocytosis (49). We showed that the WH2 domain of PXK did indeed bind actin *in vitro*, but the domain appeared to have little role in modulating EGFR trafficking by PXK; therefore, the actin binding of PXK might be involved in unidentified cellular functions of PXK other than membrane trafficking. Regarding the proline-rich motif preceding the WH2 domain at the C terminus, many proline-rich proteins are implicated in actin cytoskeletal organization, including PXK, and many share a filamentous or globular actin-binding domain. Proline-rich motifs provide binding sites for appropriate partner molecules, such as profilin, which often exists as a complex with globular actin. The motif has also been shown to interact with cortactin, an Arp2/3 complex activator, enhancing cortactin-mediated actin polymerization in the case of MIM (40). The motifs can also act as hinges with structural flexibility (28). Taken together, the data indicate that PXK might have some role in actin cytoskeletal reorganization by delivering actin monomers to the sites of polymerization or sequestering actin monomers at the sites of depolymerization in concert with proline-rich motif-binding partners. The function of PXK in actin cytoskeletal reorganization is under investigation.

PXK and receptor trafficking. We demonstrated here that PXK accelerated ligand-induced EGFR endocytosis and degradation using both exogenous expression and RNAi-mediated knockdown approaches. A series of PX domain-containing proteins have been reported to be implicated in various steps of membrane trafficking, although the underlying molecular mechanisms vary among the molecules and remain largely unclear. Among them, a relatively well-investigated molecule is SNX1. Recent studies using RNAi suggested that the feasible function of endogenous SNX1 is, by targeting to the tubular subdomain of the early endosome, to retrieve proteins from sorting endosomes to the trans-Golgi network (TGN) away from degradative lysosomal sorting by functioning as a component of retromer (3, 7, 18, 48). Another well-investigated

sorting nexin, SNX9, has been implicated in endocytosis by cooperatively functioning together with several binding partners, for example, dynamin, WASP, clathrin, AP-2, ACK1, SOS, synaptojanin, and others (4, 41, 43, 58, 62, 68, 69). The proposed function of SNX13 (RGS-PX1) is, by forming a complex with Hrs and Gαs, to promote the sorting of ubiquitinated EGFR into luminal vesicles of the multivesicular body to facilitate degradation of the receptor (71). Phospholipase D was shown to accelerate receptor endocytosis through intrinsic dynamin GTPase-activating activity of the PX domain (39). KIF16B, which associates with early endosomes through the PX domain located in its C terminus, has been reported to regulate plus-end motility of early endosomes along microtubules with its kinesin motor and to modulate the balance between receptor recycling and degradation (27). SNX16, directly interacting with EGFR, has been implicated in early/sorting endosomes to late endosomal trafficking of the receptor (9, 22). As the mechanism by which PXK modulates receptor trafficking is not clear, except for the promotion of ubiquitination of EGFR, it is important to identify the partner molecule(s) with or through which PXK modifies receptor trafficking. Since we could detect no coimmunoprecipitation of EGFR with PXK from stimulated or unstimulated COS7 cell lysates, the effect of PXK on receptor internalization and trafficking did not seem to be mediated by direct interaction with EGFR as with SNX16 (9). It would also be worth examining if PXK modulates membrane trafficking analogously to other PX domain-containing proteins, for example, acceleration of dynamin GTPase activity as with SNX9 or PLD (39, 62). Although the actin binding of PXK seemed to have little role in EGFR trafficking in our immunocytochemical experiments, we could still speculate on a role for actin binding in receptor trafficking. For example, since disassembly of polymerized actin following internalization of vesicles is a necessary step for fusion and maturation to endosomes (13), PXK might be implicated in the promotion of endocytosis by sequestering depolymerized actin monomers. Alternatively, as mentioned above, PXK could promote actin-mediated membrane invagination by delivering actin monomers to the sites of polymerization. Thus, further study should be performed before concluding that the actin binding of PXK is not involved in the modulation of receptor trafficking.

Potentiation of EGFR ubiquitination by PXK would be a primary cause for PXK to promote the receptor degradation, since it has been widely accepted that EGFR ubiquitination is an essential event for lysosomal targeting of the receptor leading to degradation (30). Suppression of the degradation by a lysosomal inhibitor supports the notion. We also observed an increase of the receptor internalization, which would also result directly from the ubiquitination of EGFR potentiated by PXK, because it has been reported that the receptor ubiquitination itself could function as a signal to initiate the internalization (20) by providing a binding site (for example, Eps15) for the machinery required for endocytosis. However, there is an opposite report that ubiquitination is not necessary for ligand-induced EGFR internalization (29). Even in this case, the enhancement of ESCRT-dependent sorting of the receptor at the endosome facilitates internalization for the next activated receptors, thus indirectly leading to acceleration of the receptor internalization. Further experiments are apparently needed to clarify the molecular mechanism by which PXK promotes EGFR ubiquitination and to define the entry and exit kinetics of internalized EGFR through the early endosome and late endosome/lysosome.

In conclusion, we isolated a protein bearing multiple domains, including a PX domain, a kinase-like domain, a proline-rich region, and a WH2 domain, and have shown that PXK is implicated in EGFR trafficking, probably through the promotion of ubiquitination. It is necessary to identify additional interacting molecules to clarify the underlying molecular mechanisms by which PXK modulates ubiquitination of EGFR and is involved in receptor trafficking. Other PX domain-containing proteins, such as $p40^{phox}$, $p47^{phox}$, CISK, C2-PI3K, and PLD, have been well characterized according to their physiological roles in cellular function in addition to their roles in membrane trafficking (54, 67). Therefore, it is possible that PXK also participates in a variety of cellular functions, such as cell migration by modulating actin cytoskeletal reorganization, as well as membrane trafficking. Interestingly, the single-nucleotide polymorphism (SNP) rs6445975 in *PXK* at chromosome 3p14.3 has recently been reported to strongly correlate with the incidence of systemic lupus erythematosis, as a result of a large genetic association study (23), suggesting that PXK has an important role in the immune system.

ACKNOWLEDGMENTS

We are grateful to members of the Cantley laboratory for critical comments, and we thank Tsuyoshi Matsuo and Seth J. Field for providing the plasmids to express EGFP-FYVE3 and GST-p40PX, respectively.

This work was supported in part by a Grant-in-Aid for Scientific Research from the Ministry of Education, Culture, Sports, Science, and Technology of Japan (to H.T. and M.H.) and by National Institutes of Health grants GM56203 and GM41890 (to L.C.C.). G.J. is the recipient of a scholarship from The Iwadare Scholarship and The Kobayashi International Scholarship Foundation.

REFERENCES

1. **Ago, T., F. Kuribayashi, H. Hiroaki, R. Takeya, T. Ito, D. Kohda, and H. Sumimoto.** 2003. Phosphorylation of p47phox directs phox homology domain from SH3 domain toward phosphoinositides, leading to phagocyte NADPH oxidase activation. Proc. Natl. Acad. Sci. U. S. A. **100:**4474–4479.
2. **Alwan, H. A., E. J. van Zoelen, and J. E. van Leeuwen.** 2003. Ligand-induced lysosomal epidermal growth factor receptor (EGFR) degradation is preceded by proteasome-dependent EGFR de-ubiquitination. J. Biol. Chem. **278:**35781–35790.
3. **Arighi, C. N., L. M. Hartnell, R. C. Aguilar, C. R. Haft, and J. S. Bonifacino.** 2004. Role of the mammalian retromer in sorting of the cation-independent mannose 6-phosphate receptor. J. Cell Biol. **165:**123–133.
4. **Badour, K., M. K. McGavin, J. Zhang, S. Freeman, C. Vieira, D. Filipp, M. Julius, G. B. Mills, and K. A. Siminovitch.** 2007. Interaction of the Wiskott-Aldrich syndrome protein with sorting nexin 9 is required for CD28 endocytosis and cosignaling in T cells. Proc. Natl. Acad. Sci. U. S. A. **104:**1593–1598.
5. **Boudeau, J., D. Miranda-Saavedra, G. J. Barton, and D. R. Alessi.** 2006. Emerging roles of pseudokinases. Trends Cell Biol. **16:**443–452.
6. **Bravo, J., D. Karathanassis, C. M. Pacold, M. E. Pacold, C. D. Ellson, K. E. Anderson, P. J. Butler, I. Lavenir, O. Perisic, P. T. Hawkins, L. Stephens, and R. L. Williams.** 2001. The crystal structure of the PX domain from p40(phox) bound to phosphatidylinositol 3-phosphate. Mol. Cell **8:**829–839.
7. **Carlton, J., M. Bujny, B. J. Peter, V. M. Oorschot, A. Rutherford, H. Mellor, J. Klumperman, H. T. McMahon, and P. J. Cullen.** 2004. Sorting nexin-1 mediates tubular endosome-to-TGN transport through coincidence sensing of high-curvature membranes and 3-phosphoinositides. Curr. Biol. **14:**1791–1800.
8. **Carlton, J., M. Bujny, A. Rutherford, and P. Cullen.** 2005. Sorting nexins—unifying trends and new perspectives. Traffic **6:**75–82.
9. **Choi, J. H., W. P. Hong, M. J. Kim, J. H. Kim, S. H. Ryu, and P. G. Suh.** 2004. Sorting nexin 16 regulates EGF receptor trafficking by phosphatidylinositol-3-phosphate interaction with the Phox domain. J. Cell Sci. **117:**4209–4218.

10. **Dumas, J. J., E. Merithew, E. Sudharshan, D. Rajamani, S. Hayes, D. Lawe, S. Corvera, and D. G. Lambright.** 2001. Multivalent endosome targeting by homodimeric EEA1. Mol. Cell **8:**947–958.
11. **Ellson, C. D., S. Andrews, L. R. Stephens, and P. T. Hawkins.** 2002. The PX domain: a new phosphoinositide-binding module. J. Cell Sci. **115:**1099–1105.
12. **Engqvist-Goldstein, A. E., and D. G. Drubin.** 2003. Actin assembly and endocytosis: from yeast to mammals. Annu. Rev. Cell Dev. Biol. **19:**287–332.
13. **Fernandez-Borja, M., L. Janssen, D. Verwoerd, P. Hordijk, and J. Neefjes.** 2005. RhoB regulates endosome transport by promoting actin assembly on endosomal membranes through Dia1. J. Cell Sci. **118:**2661–2670.
14. **Fukuda, M., and T. S. Kuroda.** 2002. Slac2-c (synaptotagmin-like protein homologue lacking C2 domains-c), a novel linker protein that interacts with Rab27, myosin Va/VIIa, and actin. J. Biol. Chem. **277:**43096–43103.
15. **Gaullier, J. M., A. Simonsen, A. D'Arrigo, B. Bremnes, H. Stenmark, and R. Aasland.** 1998. FYVE fingers bind PtdIns(3)P. Nature **394:**432–433.
16. **Giot, L., J. S. Bader, C. Brouwer, A. Chaudhuri, B. Kuang, Y. Li, Y. L. Hao, C. E. Ooi, B. Godwin, E. Vitols, G. Vijayadamodar, P. Pochart, H. Machineni, M. Welsh, Y. Kong, B. Zerhusen, R. Malcolm, Z. Varrone, A. Collis, M. Minto, S. Burgess, L. McDaniel, E. Stimpson, F. Spriggs, J. Williams, K. Neurath, N. Ioime, M. Agee, E. Voss, K. Furtak, R. Renzulli, N. Aanensen, S. Carrolla, E. Bickelhaupt, Y. Lazovatsky, A. DaSilva, J. Zhong, C. A. Stanyon, R. L. Finley, Jr., K. P. White, M. Braverman, T. Jarvie, S. Gold, M. Leach, J. Knight, R. A. Shimkets, M. P. McKenna, J. Chant, and J. M. Rothberg.** 2003. A protein interaction map of Drosophila melanogaster. Science **302:**1727–1736.
17. **Gruenberg, J.** 2001. The endocytic pathway: a mosaic of domains. Nat. Rev. Mol. Cell Biol. **2:**721–730.
18. **Haft, C. R., M. de la Luz Sierra, R. Bafford, M. A. Lesniak, V. A. Barr, and S. I. Taylor.** 2000. Human orthologs of yeast vacuolar protein sorting proteins Vps26, 29, and 35: assembly into multimeric complexes. Mol. Biol. Cell **11:**4105–4116.
19. **Haft, C. R., M. de la Luz Sierra, V. A. Barr, D. H. Haft, and S. I. Taylor.** 1998. Identification of a family of sorting nexin molecules and characterization of their association with receptors. Mol. Cell. Biol. **18:**7278–7287.
20. **Haglund, K., S. Sigismund, S. Polo, I. Szymkiewicz, P. P. Di Fiore, and I. Dikic.** 2003. Multiple monoubiquitination of RTKs is sufficient for their endocytosis and degradation. Nat. Cell Biol. **5:**461–466.
21. **Hanks, S. K., and T. Hunter.** 1995. Protein kinases 6. The eukaryotic protein kinase superfamily: kinase (catalytic) domain structure and classification. FASEB J. **9:**576–596.
22. **Hanson, B. J., and W. Hong.** 2003. Evidence for a role of SNX16 in regulating traffic between the early and later endosomal compartments. J. Biol. Chem. **278:**34617–34630.
23. **Harley, J. B., M. E. Alarcon-Riquelme, L. A. Criswell, C. O. Jacob, R. P. Kimberly, K. L. Moser, B. P. Tsao, T. J. Vyse, C. D. Langefeld, S. K. Nath, J. M. Guthridge, B. L. Cobb, D. B. Mirel, M. C. Marion, A. H. Williams, J. Divers, W. Wang, S. G. Frank, B. Namjou, S. B. Gabriel, A. T. Lee, P. K. Gregersen, T. W. Behrens, K. E. Taylor, M. Fernando, R. Zidovetzki, P. M. Gaffney, J. C. Edberg, J. D. Rioux, J. O. Ojwang, J. A. James, J. T. Merrill, G. S. Gilkeson, M. F. Seldin, H. Yin, E. C. Baechler, Q. Z. Li, E. K. Wakeland, G. R. Bruner, K. M. Kaufman, and J. A. Kelly.** 2008. Genome-wide association scan in women with systemic lupus erythematosus identifies susceptibility variants in ITGAM, PXK, KIAA1542 and other loci. Nat. Genet. **40:**204–210.
24. **Hayakawa, A., S. J. Hayes, D. C. Lawe, E. Sudharshan, R. Tuft, K. Fogarty, D. Lambright, and S. Corvera.** 2004. Structural basis for endosomal targeting by FYVE domains. J. Biol. Chem. **279:**5958–5966.
25. **Hayashi, S., T. Okada, N. Igarashi, T. Fujita, S. Jahangeer, and S. Nakamura.** 2002. Identification and characterization of RPK118, a novel sphingosine kinase-1-binding protein. J. Biol. Chem. **277:**33319–33324.
26. **Hertzog, M., C. van Heijenoort, D. Didry, M. Gaudier, J. Coutant, B. Gigant, G. Didelot, T. Preat, M. Knossow, E. Guittet, and M. F. Carlier.** 2004. The beta-thymosin/WH2 domain; structural basis for the switch from inhibition to promotion of actin assembly. Cell **117:**611–623.
27. **Hoepfner, S., F. Severin, A. Cabezas, B. Habermann, A. Runge, D. Gillooly, H. Stenmark, and M. Zerial.** 2005. Modulation of receptor recycling and degradation by the endosomal kinesin KIF16B. Cell **121:**437–450.
28. **Holt, M. R., and A. Koffer.** 2001. Cell motility: proline-rich proteins promote protrusions. Trends Cell Biol. **11:**38–46.
29. **Huang, F., L. K. Goh, and A. Sorkin.** 2007. EGF receptor ubiquitination is not necessary for its internalization. Proc. Natl. Acad. Sci. U. S. A. **104:**16904–16909.
30. **Huang, F., D. Kirkpatrick, X. Jiang, S. Gygi, and A. Sorkin.** 2006. Differential regulation of EGF receptor internalization and degradation by multiubiquitination within the kinase domain. Mol. Cell **21:**737–748.
31. **Ikonomov, O. C., D. Sbrissa, M. Foti, J. L. Carpentier, and A. Shisheva.** 2003. PIKfyve controls fluid phase endocytosis but not recycling/degradation of endocytosed receptors or sorting of procathepsin D by regulating multivesicular body morphogenesis. Mol. Biol. Cell **14:**4581–4591.
32. **Irie, H. Y., R. V. Pearline, D. Grueneberg, M. Hsia, P. Ravichandran, N. Kothari, S. Natesan, and J. S. Brugge.** 2005. Distinct roles of Akt1 and Akt2 in regulating cell migration and epithelial-mesenchymal transition. J. Cell Biol. **171:**1023–1034.
33. **Jang, I. H., S. Lee, J. B. Park, J. H. Kim, C. S. Lee, E. M. Hur, I. S. Kim, K. T. Kim, H. Yagisawa, P. G. Suh, and S. H. Ryu.** 2003. The direct interaction of phospholipase C-gamma 1 with phospholipase D2 is important for epidermal growth factor signaling. J. Biol. Chem. **278:**18184–18190.
34. **Jeng, R. L., and M. D. Welch.** 2001. Cytoskeleton: actin and endocytosis—no longer the weakest link. Curr. Biol. **11:**R691–694.
35. **Kaksonen, M., C. P. Toret, and D. G. Drubin.** 2006. Harnessing actin dynamics for clathrin-mediated endocytosis. Nat. Rev. Mol. Cell Biol. **7:**404–414.
36. **Kanai, F., H. Liu, S. J. Field, H. Akbary, T. Matsuo, G. E. Brown, L. C. Cantley, and M. B. Yaffe.** 2001. The PX domains of p47phox and p40phox bind to lipid products of PI(3)K. Nat. Cell Biol. **3:**675–678.
37. **Katzmann, D. J., G. Odorizzi, and S. D. Emr.** 2002. Receptor downregulation and multivesicular-body sorting. Nat. Rev. Mol. Cell Biol. **3:**893–905.
38. **Kurten, R. C., D. L. Cadena, and G. N. Gill.** 1996. Enhanced degradation of EGF receptors by a sorting nexin, SNX1. Science **272:**1008–1010.
39. **Lee, C. S., I. S. Kim, J. B. Park, M. N. Lee, H. Y. Lee, P. G. Suh, and S. H. Ryu.** 2006. The phox homology domain of phospholipase D activates dynamin GTPase activity and accelerates EGFR endocytosis. Nat. Cell Biol. **8:**477–484.
40. **Lin, J., J. Liu, Y. Wang, J. Zhu, K. Zhou, N. Smith, and X. Zhan.** 2005. Differential regulation of cortactin and N-WASP-mediated actin polymerization by missing in metastasis (MIM) protein. Oncogene **24:**2059–2066.
41. **Lin, Q., C. G. Lo, R. A. Cerione, and W. Yang.** 2002. The Cdc42 target ACK2 interacts with sorting nexin 9 (SH3PX1) to regulate epidermal growth factor receptor degradation. J. Biol. Chem. **277:**10134–10138.
42. **Liu, L., C. Yang, J. Yuan, X. Chen, J. Xu, Y. Wei, J. Yang, G. Lin, and L. Yu.** 2005. RPK118, a PX domain-containing protein, interacts with peroxiredoxin-3 through pseudo-kinase domains. Mol. Cells **19:**39–45.
43. **Lundmark, R., and S. R. Carlsson.** 2003. Sorting nexin 9 participates in clathrin-mediated endocytosis through interactions with the core components. J. Biol. Chem. **278:**46772–46781.
44. **Lunn, M. L., R. Nassirpour, C. Arrabit, J. Tan, I. McLeod, C. M. Arias, P. E. Sawchenko, J. R. Yates III, and P. A. Slesinger.** 2007. A unique sorting nexin regulates trafficking of potassium channels via a PDZ domain interaction. Nat. Neurosci. **10:**1249–1259.
45. **Mao, H., T. S. Ferguson, S. M. Cibulsky, M. Holmqvist, C. Ding, H. Fei, and I. B. Levitan.** 2005. MONaKA, a novel modulator of the plasma membrane Na, K-ATPase. J. Neurosci. **25:**7934–7943.
46. **McPherson, P. S.** 1999. Regulatory role of SH3 domain-mediated protein-protein interactions in synaptic vesicle endocytosis. Cell Signal. **11:**229–238.
47. **Mellman, I.** 1996. Endocytosis and molecular sorting. Annu. Rev. Cell Dev. Biol. **12:**575–625.
48. **Merino-Trigo, A., M. C. Kerr, F. Houghton, A. Lindberg, C. Mitchell, R. D. Teasdale, and P. A. Gleeson.** 2004. Sorting nexin 5 is localized to a subdomain of the early endosomes and is recruited to the plasma membrane following EGF stimulation. J. Cell Sci. **117:**6413–6424.
49. **Paavilainen, V. O., E. Bertling, S. Falck, and P. Lappalainen.** 2004. Regulation of cytoskeletal dynamics by actin-monomer-binding proteins. Trends Cell Biol. **14:**386–394.
50. **Parks, W. T., D. B. Frank, C. Huff, C. Renfrew Haft, J. Martin, X. Meng, M. P. de Caestecker, J. G. McNally, A. Reddi, S. I. Taylor, A. B. Roberts, T. Wang, and R. J. Lechleider.** 2001. Sorting nexin 6, a novel SNX, interacts with the transforming growth factor-beta family of receptor serine-threonine kinases. J. Biol. Chem. **276:**19332–19339.
51. **Patki, V., D. C. Lawe, S. Corvera, J. V. Virbasius, and A. Chawla.** 1998. A functional PtdIns(3)P-binding motif. Nature **394:**433–434.
52. **Paunola, E., P. K. Mattila, and P. Lappalainen.** 2002. WH2 domain: a small, versatile adapter for actin monomers. FEBS Lett. **513:**92–97.
53. **Ponting, C. P.** 1996. Novel domains in NADPH oxidase subunits, sorting nexins, and PtdIns 3-kinases: binding partners of SH3 domains? Protein Sci. **5:**2353–2357.
54. **Sato, T. K., M. Overduin, and S. D. Emr.** 2001. Location, location, location: membrane targeting directed by PX domains. Science **294:**1881–1885.
55. **Schafer, D. A.** 2002. Coupling actin dynamics and membrane dynamics during endocytosis. Curr. Opin. Cell Biol. **14:**76–81.
56. **Scheeff, E. D., and P. E. Bourne.** 2005. Structural evolution of the protein kinase-like superfamily. PLoS Comput. Biol. **1:**e49.
57. **Schopperle, W. M., M. H. Holmqvist, Y. Zhou, J. Wang, Z. Wang, L. C. Griffith, I. Keselman, F. Kusinitz, D. Dagan, and I. B. Levitan.** 1998. Slob, a novel protein that interacts with the Slowpoke calcium-dependent potassium channel. Neuron **20:**565–573.
58. **Schulze, W. X., and M. Mann.** 2004. A novel proteomic screen for peptide-protein interactions. J. Biol. Chem. **279:**10756–10764.
59. **Seet, L. F., and W. Hong.** 2006. The Phox (PX) domain proteins and membrane traffic. Biochim. Biophys. Acta **1761:**878–896.
60. **Slagsvold, T., A. Marchese, A. Brech, and H. Stenmark.** 2006. CISK attenuates degradation of the chemokine receptor CXCR4 via the ubiquitin ligase AIP4. EMBO J. **25:**3738–3749.

61. **Sorkin, A., and L. K. Goh.** 2009. Endocytosis and intracellular trafficking of ErbBs. Exp. Cell Res. **315:**683–696.
62. **Soulet, F., D. Yarar, M. Leonard, and S. L. Schmid.** 2005. SNX9 regulates dynamin assembly and is required for efficient clathrin-mediated endocytosis. Mol. Biol. Cell **16:**2058–2067.
63. **Stenmark, H., and D. J. Gillooly.** 2001. Intracellular trafficking and turnover of phosphatidylinositol 3-phosphate. Semin. Cell Dev. Biol. **12:**193–199.
64. **Vergarajauregui, S., A. San Miguel, and R. Puertollano.** 2006. Activation of p38 mitogen-activated protein kinase promotes epidermal growth factor receptor internalization. Traffic **7:**686–698.
65. **Worby, C. A., and J. E. Dixon.** 2002. Sorting out the cellular functions of sorting nexins. Nat. Rev. Mol. Cell Biol. **3:**919–931.
66. **Xing, Y., D. Liu, R. Zhang, A. Joachimiak, Z. Songyang, and W. Xu.** 2004. Structural basis of membrane targeting by the Phox homology domain of cytokine-independent survival kinase (CISK-PX). J. Biol. Chem. **279:**30662–30669.
67. **Xu, Y., L. F. Seet, B. Hanson, and W. Hong.** 2001. The Phox homology (PX) domain, a new player in phosphoinositide signalling. Biochem. J. **360:**513–530.
68. **Yarar, D., C. M. Waterman-Storer, and S. L. Schmid.** 2007. SNX9 couples actin assembly to phosphoinositide signals and is required for membrane remodeling during endocytosis. Dev. Cell **13:**43–56.
69. **Yeow-Fong, L., L. Lim, and E. Manser.** 2005. SNX9 as an adaptor for linking synaptojanin-1 to the Cdc42 effector ACK1. FEBS Lett. **579:**5040–5048.
70. **Zeng, H., H. Fei, and I. B. Levitan.** 2004. The slowpoke channel binding protein Slob from Drosophila melanogaster exhibits regulatable protein kinase activity. Neurosci. Lett. **365:**33–38.
71. **Zheng, B., C. Lavoie, T. D. Tang, P. Ma, T. Meerloo, A. Beas, and M. G. Farquhar.** 2004. Regulation of epidermal growth factor receptor degradation by heterotrimeric Galphas protein. Mol. Biol. Cell **15:**5538–5550.
72. **Zheng, B., Y. C. Ma, R. S. Ostrom, C. Lavoie, G. N. Gill, P. A. Insel, X. Y. Huang, and M. G. Farquhar.** 2001. RGS-PX1, a GAP for GalphaS and sorting nexin in vesicular trafficking. Science **294:**1939–1942.
73. **Zhong, Q., C. S. Lazar, H. Tronchere, T. Sato, T. Meerloo, M. Yeo, Z. Songyang, S. D. Emr, and G. N. Gill.** 2002. Endosomal localization and function of sorting nexin 1. Proc. Natl. Acad. Sci. U. S. A. **99:**6767–6772.
74. **Zhong, Q., M. J. Watson, C. S. Lazar, A. M. Hounslow, J. P. Waltho, and G. N. Gill.** 2005. Determinants of the endosomal localization of sorting nexin 1. Mol. Biol. Cell **16:**2049–2057.
75. **Zou, X., G. Qiu, C. Chen, M. Wu, Y. Hu, H. Zheng, X. Li, S. Gu, C. Ji, and Y. Mao.** 2005. Expression pattern and subcellular localization of five splice isoforms of human PXK. Int. J. Mol. Med. **16:**701–707.